Precision native polysaccharides from living polymerization of anhydrosugars

Lianqian Wu[1], Zefeng Zhou[1], Devavrat Sathe[2], Junfeng Zhou[2], Shoshana Reich[1], Zhensheng Zhao[1], Junpeng Wang[2], Jia Niu[1]*

1. Department of Chemistry, Boston College, Chestnut Hill, Massachusetts 02467, United States
2. School of Polymer Science and Polymer Engineering, University of Akron, Akron, Ohio 44325, United States

* Correspondence to: jia.niu@bc.edu

The composition, sequence, length, and type of glycosidic linkages of polysaccharides profoundly affect their biological and physical properties. However, investigation of the structure-function relationship of polysaccharides is hampered by accessing well-defined polysaccharides in sufficient quantities. Here, we report a chemical approach to precision polysaccharides with native glycosidic linkages via living cationic ring-opening polymerization of 1,6-anhydrosugars. We synthesized well-defined polysaccharides with tunable molecular weight, low dispersity, and excellent regio- and stereoselectivity using a boron trifluoride etherate catalyst and glycosyl fluoride initiators. Computational studies revealed that the reaction propagated through the monomer α-addition to the oxocarbenium and was controlled by the reversible deactivation of the propagating oxocarbenium to form the glycosyl fluoride dormant species. Our method afforded a facile and scalable pathway to multiple biologically relevant precision polysaccharides, including D-glucan, D-mannan, and

an unusual L-glucan. We demonstrated that catalytic depolymerization of precision polysaccharides efficiently regenerated monomers, suggesting their utility as a class of chemically recyclable materials with tailored thermal and mechanical properties.

Polysaccharides are among the most abundant biopolymers on Earth. In addition to their essential functions in biology[1], the utilization of polysaccharide-based biomass in renewable energy[2] and sustainable materials[3] is also critical to reducing carbon emissions worldwide. However, polysaccharides isolated from biological sources are often heterogeneous[4], imposing significant constraints on their characterization and utilization for emerging technologies. Therefore, the development of synthetic approaches to polysaccharides has been one of the main research areas in glycoscience[5]. For example, enzymatic synthesis has emerged as a promising method for polysaccharide synthesis owing to the perfect regio- and stereoselectivity of the enzymatic glycosylation, and the elimination of the need for protecting groups[6]. However, limited enzyme availability and high specificity generally restrict them to specific substrates or reactions. Iterative assembly strategies have been developed to prepare synthetic polysaccharides with precise sequence and length[7]. Notably, the automated glycan assembly (AGA) techniques developed by Seeberger has enabled the construction of complex polysaccharides (Fig. 1a)[8-9]. Nevertheless, the stepwise assembly methods require significant investments in equipment and reagents, and often have modest scalability.

Chemical polymerization is an efficient method for the scalable synthesis of polysaccharides and glycomimetic polymers[10]. Over the last ten years, many carbohydrate-derived monomers have been used to generate carbohydrate polymers, such as isosorbide[11], xylose[12], isohexide[13], and levoglucosenyl ether[14] (Fig. 1a). Particularly worth noting are the living anionic ring-opening

polymerization of monosaccharide-derived cyclic carbonate and β-lactam reported by Wooley[15] and Grinstaff[16], respectively. However, these polymers all consist of non-glycosidic linkages, and in some cases, control over the polymerization remains challenging. While the cationic ring-opening polymerization (CROP) of 1,6-anhydrosugars has been employed to produce polysaccharides since the 1960s[17], achieving control over this polymerization remains a formidable challenge. In this work, we leveraged the synergistic combination of a glycosyl donor initiator and a mild Lewis acid catalyst to achieve *living* CROP of 1,6-anhydrosugars (Fig. 1b). Native polysaccharides with controlled molecular weight and excellent regio- and stereoselectivity could be readily prepared from these biorenewable monomers. Our proposed mechanism is centered on reversible deactivation of the propagating oxocarbenium[18], which is generated by the fluoride abstraction from glycosyl fluoride initiator by boron trifluoride catalyst. Addition of the 1,6-anhydrosugar monomer to oxocarbenium from the less sterically demanding α-face affords an α-oxonium[19]. Followed by a rapid ring opening process, the oxocarbenium was regenerated. An equilibrium between oxocarbenium species and dormant glycosyl fluoride is established to achieve controlled chain growth (Fig. 1c). It is worth noting that Coates et al. recently harnessed a similar strategy to accomplish the controlled polymerization of cyclic acetals[20].

Results and discussion

Preparation and characterization of precision polysaccharides. From the outset, *O*-methylated 1,6-anhydro-β-D-glucopyranose **Me-D-Glc** was utilized as a model monomer, which can be readily obtained after a one-step methylation of the biomass-derived and commercially available 1,6-anhydro-β-D-glucopyranose ($1.3/g) in high yield and decagram scale (94%, 11.8 g). Previous works by Kamigaito[21] and Fors[22] have shown that thiocarbamate chain transfer agents could

regulate the propagation of oxocarbenium ions, which are structurally like the proposed propagating species in the polymerization of 1,6-anhydrosugars (Fig. 1c). Separately, glycosyl thiocarbamate also served as a good glycosyl donor in catalytic glycosylation reactions[23]. Based on these seminal reports, a series of glycosyl donors were evaluated, including glycosyl thiocarbamate **I-1**, glycosyl trithiocarbonate **I-S1**, and glycosyl xanthate **I-S2**, for their ability to initiate the CROP of 1,6-anhydrosugars by mild Lewis acid catalysts (Supplementary Table 1). While **I-1** in conjunction with $Cu(OTf)_2$ produced a polysaccharide with a number-average molecular weight (M_n) of 6.9 kg/mol, the high dispersity ($Đ$ = 1.54) and the low fidelity of the ω-chain end suggested poor control over the polymerization (Fig. 2a (i)). We attributed the low level of control to the lability of C–S bond in these glycosyl donors under acidic condition and hypothesized that more stable glycosyl donors could lead to improved control. Indeed, glycosyl chloride **I-2** was found to afford a polysaccharide with a 60% fidelity of the ω-chain end (Fig. 2a (ii)). Encouragingly, a more stable glycosyl fluoride **I-3** provided an excellent ω-chain end fidelity (90%) when boron trifluoride etherate (BF_3•Et_2O) was used as the catalyst (Fig. 2a (iii) and Supplementary Fig. 57). Size-exclusion chromatography (SEC) analysis of the sample, **P(Me-D-Glc)**, revealed a monomodal molar mass distribution with a dispersity ($Đ$) of 1.23 (Supplementary Fig. 44). The number-average molecular weight (M_n) calculated based on the ^{1}H NMR analysis (9.5 kg/mol) agreed well with the theoretical value (8.7 kg/mol) (Fig. 3a, entry 1). In addition, the chain-end groups were confirmed by matrix assisted laser desorption/ionization-time-of-flight (MALDI-TOF) mass spectroscopy (Fig. 2b). The well-defined structure of **P(Me-D-Glc)**, including the α-, ω-chain ends and α-1,6-glucan backbone, was further demonstrated by ^{1}H NMR (Fig. 2c) and ^{19}F NMR analyses (Supplementary Fig. 59). Notably, the single anomeric carbon signal at 96.34 ppm in ^{13}C NMR (Supplementary Fig. 58) and the high positive specific rotation

of $[\alpha]_D^{20} = +201.3°$ unambiguously supported that **P(Me-D-Glc)** was highly stereoregular[24], i.e., α-glycosidic linkages were exclusively generated. The polymerization also displayed characteristics consistent with living polymerization, including first-order reaction kinetics, linear growth of the molecular weights over conversion, controlled molecular weights proportional to $[M]_0/[I]_0$ ratio, and low dispersity (Fig. 2d).

Monomer scope. With the initiator/catalyst pair identified, we then sought to explore the monomer scope of this polymerization (Fig. 3a). *O*-alkylated 1,6-anhydrosugars with various alkyl side chains, including ethyl, *n*-propyl, *n*-butyl, *n*-pentyl, and allyl all exhibited good reactivities and excellent control over the polymerization (Fig. 3a, entry 2-6). Notably, ^{1}H, ^{13}C NMR, and high positive specific rotation values consistently supported exclusive α-1,6-D-glycosidic linkages in these polysaccharides (see Supplementary Information for details). Remarkably, a polysaccharide with a degree of polymerization (DP) of 185 was obtained with relatively low dispersity ($Đ$ = 1.38) when *O*-ethyl monomer **Et-D-Glc** was polymerized (Fig. 3a, entry 2). For the 1,6-anhydrosugars with long *O*-alkyl side chains (*e.g.*, *n*-butyl and *n*-pentyl), the addition of external fluoride ions further improved control over the polymerization (Fig. 3a, entry 4-5). Furthermore, this methodology was not limited to 1,6-anhydroglucose. *O*-allyl 1,6-anhydromannose **All-D-Man** and *O*-ethyl 1,6-anhydrogalactose **Et-D-Gal** could also be polymerized with high efficiency and excellent control (Fig. 3a, entry 9-10), yielding well-defined α-1,6-polymannose and α-1,6-polygalactose, respectively.

Computational investigations. Density functional theory (DFT) calculations were performed to gain more mechanistic insights into the reversible deactivation process in the living CROP and the

origin of the excellent α-selectivity during the propagation step (Fig. 3b). The energy surface of activation of the dormant glycosyl fluoride **1** was first calculated, showing that the reaction readily gave an active oxocarbenium species **2** with an energy barrier of 7.1 kcal mol^{-1}. The facile activation of glycosyl fluoride chain end was attributed to the hardness of the fluorine atom, making it more readily to be abstracted by hard Lewis acid boron trifluoride. On the other hand, the reverse reaction, namely the deactivation of oxocarbenium species **2** by BF_4^- counterion, occurred with a low energy barrier of 4.4 kcal mol^{-1}, and the fast deactivation process might arise from the strong anomeric effect of the glycosyl fluoride. In short, the synergy of glycosyl fluoride and boron trifluoride results in an equilibrium between the active and dormant species, with the ratio of propagating oxocarbenium : dormant species being 0.01. The low concentration of the propagating oxocarbenium results in livingness in the polymerization.

As for the propagation process, two sequential steps were then considered. A monomer first attacked the oxocarbenium to form an oxonium species **3**, and then a subsequent ring opening reaction occurred to regenerate the propagating oxocarbenium. According to the DFT calculations, the energy barrier of the α-addition was lower than that of the β-addition ($TS_{2\_3\alpha}$ = 4.9 kcal mol^{-1} versus $TS_{2\_3\beta}$ = 9.9 kcal mol^{-1}). The difference in transition state energies is primarily attributed to the steric repulsion between the incoming anhydrosugar monomer and oxocarbenium species. This α-selectivity is consistent with the experimental results, where the single anomeric carbon signal was observed in ^{13}C NMR spectra of the precision polysaccharides. A ring opening process was identified after the formation of oxonium intermediate **3α**, which is considerably exergonic by 6.7 kcal mol^{-1}, indicative of the facile regeneration of the oxocarbenium. It is noteworthy that the direct addition to oxonium **3α** by the anhydrosguar monomer proposed by Schuerch[17] yielded no

computationally viable transition states despite extensive searches. This result is consistent with a recent work by Reineke[19].

Chain extension and chain end modifications. Synthesizing advanced polymeric architectures, such as block copolymers, represents one of the greatest advantages of living polymerization. Building upon this method, we attempted to access block copolysaccharides that are otherwise laborious to synthesize. First, polymerization of **^{n}Bu-D-Glc** was carried out in the presence of **I-3** to give a macroinitiator **P(^{n}Bu-D-Glc)** (M_n = 3.2 kg/mol, $Đ$ = 1.15) with an excellent fidelity of the ω-chain end (Supplementary Fig. 3). Next, chain extension of **P(^{n}Bu-D-Glc)** by **Me-D-Glc** yielded a diblock copolysaccharide P(**^{n}Bu-D-Glc**)-***b***-P(**Me-D-Glc**). A shift to higher molecular weight, monomodal distribution with low $Đ$ (1.17) and little to no tailing in SEC traces (Fig. 2e), as well as a single peak in the diffusion-ordered spectroscopy (DOSY) NMR analysis (Supplementary Fig. 6) firmly supported the successful chain-extension.

Furthermore, as glycosyl fluoride has been widely used as a glycosyl donor in catalytic glycosylation reactions, the ω-F chain end presents a versatile handle for further functionalization. As a proof of this principle, glycosylation of alkenyl and alkynyl alcohol by the ω-F chain end of **P(Me-D-Glc)** was examined using BF_3•Et_2O as an activator (Fig. 2f). The ^{1}H NMR and MALDI-TOF MS analyses indicated that the transformations of ω-F chain end were quantitative (Supplementary Fig. 10-13), creating an opportunity for the post-polymerization functionalization of precision polysaccharides via thiol-ene and Cu(I)-catalyzed azide-alkyne cycloaddition (CuAAC) click chemistries.

Synthesis of native polysaccharides. Oligomeric α-1,6-glycans play significant roles in many biological processes[25]. Therefore, we sought to apply the current polymerization method to access these biologically important glycans. Because of the facile removal of allyl groups, *O*-allyl 1,6-D-anhydroglucose **All-D-Glc** was chosen as the monomer. Polymerization of **All-D-Glc** at $[M]_0$:$[I]_0$ ratio of 10:1 yielded a precision polysaccharide **P**(**All-D-Glc**) with excellent molecular weight control (Fig. 3a, entry 6). Notably, this synthetic procedure was readily scalable (Fig. 4a): 1.1 grams of precise polysaccharide **P**(**All-D-Glc**) was obtained without loss of control as indicated by a monomodal SEC peak and low *Đ* (1.24). Followed by Pd-catalyzed deprotection, a well-defined α-1,6-D-glucan **P**(**OH-D-Glc**) was prepared. The obtained α-1,6-D-glucan showed identical ^{1}H NMR and ^{13}C NMR spectra to the natural α-1,6-D-glucan (Fig. 4a and Supplementary Fig. 20), which further verified the excellent regio- and stereoselectivity of this method. Importantly, the ω-F chain end was still observed in synthetic glucan, which could potentially be used as a glycosyl donor in enzymatic glycosylation to access more complex glycans[26].

Biosynthetic pathways of polysaccharides predominantly produce D-enantiomers which are susceptible to enzymatic degradation[27]. In contrast, a chemical polymerization process does not discriminate either D- or L-anhydrosugars, providing a good opportunity to generate physiologically stable all-L-polysaccharides. Indeed, in the presence of a L-glycosyl fluoride initiator ***ent*-I-3**, 1,6-anhydro-β-L-glucopyranose **^{n}Bu-L-Glc** and **All-L-Glc** could be polymerized to give the corresponding all-L-polysaccharide without any erosion in efficiency and livingness (Fig. 3a, entry 7-8). Applying the same deprotection protocol to **P(All-L-Glc)**, a rare α-1,6-L-glucan was obtained. Equal but opposite-in-sign specific rotation values were observed for D- and L-glucans (Fig. 4b), confirming the stereoregularity and enantiopurity of both polysaccharides. To the best of our knowledge, the α-1,6-L-glucan prepared herein represents the first example of

precision all-L-glycans. Both D- and L-glucans were treated with dextranase from *Penicillium funiculosum*. SEC analyses of the degradation reaction revealed complete degradation of D-glucan, while L-glucan remained intact (Fig. 4b). The remarkable resistance of L-glucans against glycosidase-mediated degradation suggested their potential physiological stability for future biomedical applications.

Furthermore, we demonstrated the synthetic utility of the current living CROP strategy to synthesize α-1,6-D-mannan, a polysaccharide that exists in the cell wall of *Mycobacterium tuberculosis* and is implicated in the human immune response to pathogens[28]. To produce precision α-1,6-D-mannan, **All-D-Man** was first polymerized into a well-defined polysaccharide **P(All-D-Man)** (M_n = 3.3 kDa, $Đ$ = 1.24). After removing the allyl groups, a well-defined α-1,6-D-mannan was readily generated (Fig. 4c), which was determined to be composed of α-1,6-D-glycosidic linkages by ^{1}H and ^{13}C NMR (Supplementary Fig. 102-103). Therefore, the current polymerization pathway becomes a promising alternative to the labor/equipment-demanding stepwise glycan assembly strategies for constructing biologically relevant polysaccharides[29].

Depolymerization and repolymerization. Beyond biologically active polysaccharides, we also explored renewable materials based on precision polysaccharides. One of the most desired properties of the next-generation sustainable polymers is their inherent chemical recyclability, which enables a closed-loop life cycle[30-33]. Given that 1,6-anhydroglucose was produced by the thermolysis of starch or cellulose, we first subjected precision polysaccharide **P(Me-D-Glc)** to thermolysis conditions (450 °C, 30 mmHg). Indeed, monomer **Me-D-Glc** could be recovered in 34% yield (Supplementary Fig. 39). Despite the low yield, this result suggested the chemical recyclability of precision polysaccharides. Further thermodynamic analysis via variable-temperature ^{1}H NMR (Supplementary Fig. 38) revealed the standard state thermodynamic

parameters of the living CROP of **Et-D-Glc**: $\Delta H°$ = -26.8 kJ/mol, $\Delta S°$ = -73.1 $J \cdot mol^{-1} \cdot K^{-1}$. Correspondingly, the ceiling temperature (T_c) was calculated to be 366 K (93 °C) at $[M]_0$ = 1.0 M, suggesting that the precision polysaccharide could be catalytically depolymerized under a relatively mild condition close to the T_c. Consistent with this rationale, we found **P(Et-D-Glc)** could be quantitatively depolymerized to yield the monomer **Et-D-Glc** at 80 °C in the presence of a catalytic amount of $BF_3 \bullet Et_2O$ (Fig. 5a). Additionally, the recovered **Et-D-Glc** was repolymerized to give **P(Et-D-Glc)** with an efficiency comparable to the pristine monomer. Therefore, a circular monomer-polymer-monomer life cycle of the precision polysaccharides was demonstrated (Fig. 5a).

Material properties. Labile main-chain groups (*e.g.*, acetal, ester, enamine) are often incorporated into the existing chemically recyclable polymers to enable depolymerization[20,34-38], rendering these polymers unstable under harsh conditions (*e.g.*, strong acid/base, high temperature, etc.). In contrast, the precision polysaccharides exhibited remarkable chemical and thermal stability. Little to no change in molecular weight and dispersity was found when exposing **P(Me-D-Glc)** to an excessive amount of Brønsted acid (e.g., acetic acid or trifluoroacetic acid) or base (e.g., pyridine, triethylamine, or 1,8-diazabicyclo[5.4.0]undec-7-ene) for 24 h (Fig. 5b (i)). Thermogravimetric analysis (TGA) revealed an onset decomposition temperature T_d (defined by 5% weight loss) greater than 345°C (Fig. 5b (ii)). Impressively, the morphology and thermal performance of precision polysaccharides were readily tunable by side chain modifications. **P(Me-D-Glc)** turned out to be highly crystalline with well-defined diffraction patterns as revealed by powder X-ray diffraction (PXRD) spectrum, in which three major diffraction signals at 7.5º, 13.1º, and 18.9º were observed (Fig. 5c (i), inset). Additionally, a high melting temperature (T_m) of 284 °C was

detected in differential scanning calorimetry (DSC) analysis (Fig. 5c (i)). In contrast, a T_m was not found in the polysaccharides carrying longer alkyl groups. At the same time, their glass-transition temperatures (T_gs) changed from 67 ºC to -23 ºC when varying the *O*-alkyl substitution from ethyl to *n*-pentyl (Fig. 5c (ii)). The precision polysaccharides represent a rare example that significant changes in the polymer morphology and thermal properties can be induced by simply altering the side chains[19,39].

The chemical recyclability, together with good chemical and thermal stabilities make these polysaccharides promising candidates for sustainable materials (Fig. 5d). In particular, a copolysaccharide **PN1** consisting of 65 mol% **ⁿPen-D-Glc**, 30 mol% **Me-D-Glc**, and 5 mol% crosslinker **CL** displayed mechanical properties typical for an elastomer: a Young's modulus of 106.63 ± 16.17 MPa, a tensile strength of 4.06 ± 0.09 MPa, and elongation at break reaching 138 ± 15%. In contrast, a completely different material (**PN2**) was obtained when the copolysaccharide composition changed to 30 mol% **ⁿPen-D-Glc**, 65 mol% **Me-D-Glc**, and 5 mol% crosslinker **CL**. As a glassy material, **PN2** showed higher Young's modulus (0.82 ± 0.10 GPa) and ultimate tensile strength (19.17 ± 1.92 MPa), with elongation at break of 2.6 ± 0.3%. The drastic change in the mechanical properties was attributed to the different T_gs of **PN1** and **PN2** (22 ºC *vs*. 55 ºC)[40], which lead to elastic (**PN1**) or glassy (**PN2**) characteristics, respectively. Both copolysaccharide-based materials could be depolymerized completely (Fig. 5e), with the monomers and crosslinker recovered in excellent yield (85%). The recovered 1,6-anhydrosugars were repolymerized, and the resulting copolysaccharides **PN1'** and **PN2'** showed identical tensile properties to pristine **PN1** and **PN2**, respectively (Supplementary Fig. 42-43).

Conclusions

In conclusion, a chemical approach to precision native polysaccharides through *living polymerization* of 1,6-anhydrosugars was developed. The generality of this method enabled the facile synthesis of a variety of polysaccharides and oligo-glycans with excellent regio- and stereoselectivity, precise molecular weight control, and high fidelity of the chain end groups. In addition, the obtained materials displayed excellent chemical recyclability and tunable thermal and mechanical properties. Overall, the method presented herein created a new paradigm for the chemical synthesis of polysaccharides with strong implications in a range of applications spanning from materials science to bioengineering.

References

1. Varki, A. et al. *Essentials of Glycobiology* (Cold Spring Harbor Laboratory Press, New York, ed. 2, 2009).

2. Ragauskas, A. J. et al. The path forward for biofuels and biomaterials. *Science* **311**, 484–489 (2006).

3. Zhu, Y., Romain, C. & Williams, C. K. Sustainable polymers from renewable resources. *Nature* **540**, 354–362 (2016).

4. Dumitriu, S. *Polysaccharides: Structural Diversity and Functional Versatility* (Marcel Dekker, New York, ed. 2, 2005).

5. Fittolani, G., Tyrikos-Ergas, T., Vargová, D., Chaube, M. A. & Delbianco, M. Progress and challenges in the synthesis of sequence controlled polysaccharides. *Beilstein J. Org. Chem.* **17**, 1981–2025 (2021).

6. Kadokawa, J. Precision polysaccharide synthesis catalyzed by enzymes. *Chem. Rev.* **111**, 4308–4345 (2011).

7. Zhu, Q. et al. Chemical synthesis of glycans up to a 128-mer relevant to the O-antigen of bacteroides vulgatus. *Nat. Commun.* **11**, 4142–4148 (2020).

8. Guberman, M. & Seeberger, P. H. Automated glycan assembly: a perspective. *J. Am. Chem. Soc.* **141**, 5581–5592 (2019).

9. Panza, M., Pistorio, S. G., Stine, K. J. & Demchenko, A. V. Automated chemical oligosaccharide synthesis: novel approach to traditional challenges. *Chem. Rev.* **118**, 8105–8150 (2018).

10. Xiao, R. X. & Grinstaff, M. W. Chemical synthesis of polysaccharides and polysaccharide mimetics. *Prog. Polym. Sci.* **74**, 78–116 (2017).

11. Saxon, D. J. et al. Architectural control of isosorbide-based polyethers via ring-opening polymerization. *J. Am. Chem. Soc.* **141**, 5107–5111 (2019).

12. McGuire, T. M. et al. Control of crystallinity and stereocomplexation of synthetic carbohydrate polymers from D- and L-xylose. *Angew. Chem., Int. Ed.* **60**, 4524–4528 (2021).

13. Stubbs, C. J. et al. Sugar-based polymers with stereochemistry-dependent degradability and mechanical properties. *J. Am. Chem. Soc.* **144**, 1243–1250 (2022).

14. Debsharma, T., Yagci, Y. & Schlaad, H. Cellulose-derived functional polyacetal by cationic ring-opening polymerization of levoglucosenyl methyl ether. *Angew. Chem., Int. Ed.* **58**, 18492–18495 (2019).

15. Mikami, K. et al. Polycarbonates derived from glucose via an organocatalytic approach. *J. Am. Chem. Soc.* **135**, 6826–6829 (2013).

16. Dane, E. L. & Grinstaff, M. W. Poly-amido-saccharides: synthesis via anionic polymerization of a β-lactam sugar monomer. *J. Am. Chem. Soc.* **134**, 16255–16264 (2012).

17. Ruckel, E. R. & Schuerch, C. Preparation of high polymers from 1,6-anhydro-2,3,4-tri-*O*-substituted β-D-glucopyranose. *J. Org. Chem.* **31**, 2233–2239 (1966).

18. Aoshima, S. & Kanaoka, S. A renaissance in living cationic polymerization. *Chem. Rev.* **109**, 5245–5287 (2009).

19. Porwal, M. K. et al. Stereoregular functionalized polysaccharides via cationic ring-opening polymerization of biomass derived levoglucosan. *Chem. Sci.* **13**, 4512–4522 (2022).

20. Abel, B. A., Snyder, R. L. & Coates, G. W. Chemically recyclable thermoplastics from reversible-deactivation polymerization of cyclic acetals. *Science* **373**, 783–789 (2021).

21. Uchiyama, M., Satoh, K. & Kamigaito, M. Cationic RAFT polymerization using ppm concentrations of organic acid. *Angew. Chem., Int. Ed.* **54**, 1924–1928 (2015).

22. Kottisch, V., Michaudel, Q. & Fors, B. P. Cationic polymerization of vinyl ethers controlled by visible light. *J. Am. Chem. Soc.* **138**, 15535–15538 (2016).

23. Nielsen, M. M. & Pedersen, C. M. Catalytic glycosylations in oligosaccharide synthesis. *Chem. Rev.* **118**, 8285–8358 (2018).

24. Yoshida, D. & Yoshida, T. Elucidation of high ring-opening polymerizability of methylated 1,6-anhydro glucose. *J. Polym. Sci. A. Polym. Chem.* **47**, 1013–1022 (2009).

25. Zhu, Q. Q. et al. Structural identification of (1⟶6)-α-D-glucan, a key responsible for the health benefits of longan, and evaluation of anticancer activity. *Biomacromolecules* **14**, 1999–2003 (2013).

26. Williams, S. J. & Withers, S. G. Glycosyl fluorides in enzymatic reactions. *Carbohydr. Res.* **327**, 27–46 (2000).

27. Stone, B. A., Svensson, B., Collins, M. E. & Rastall, R. A. Polysaccharide Degradation in *Glycoscience* (Springer, Heidelberg, ed. 2, 2008), pp. 2325–2375.

28. Apostolou, I. et al. Murine natural killer cells contribute to the granulomatous reaction caused by mycobacterial cell walls. *Proc. Natl. Acad. Sci. U.S.A.* **96**, 5141–5146 (1999).

29. Calin, O., Eller, S. & Seeberger, P. H. Automated polysaccharide synthesis: assembly of a 30mer mannoside. *Angew. Chem., Int. Ed.* **52**, 5862–5865 (2013).

30. Getzler, Y. D. Y. L. & Coates, G. W. Chemical recycling to monomer for an ideal, circular polymer economy. *Nat. Rev. Mater.* **5**, 501–516 (2020).

31. Shi, C. et al. Design principles for intrinsically circular polymers with tunable properties. *Chem* **7**, 2896–2912 (2021).

32. Mohadjer Beromi, M. et al. Iron-catalysed synthesis and chemical recycling of telechelic 1,3-enchained oligocyclobutanes. *Nat. Chem.* **13**, 156–162 (2021).

33. Sathe, D. et al. Olefin metathesis-based chemically recyclable polymers enabled by fused-ring monomers. *Nat. Chem.* **13**, 743–750 (2021).

34. Hong, M. & Chen, E. Y.-X. Completely recyclable biopolymers with linear and cyclic topologies via ring-opening polymerization of γ-butyrolactone. *Nat. Chem.* **8**, 42–49 (2016).

35. Zhu, J. B., Watson, E. M., Tang, J. & Chen, E. Y.-X. A synthetic polymer system with repeatable chemical recyclability. *Science* **360**, 398–403 (2018).

36. Häußler, M., Eck, M., Rothauer, D. & Mecking, S. Closed-loop recycling of polyethylene-like materials. *Nature* **590**, 423–427 (2021).

37. Yuan, J. S. et al. *J. Am. Chem. Soc.* **141**, 4928–4935 (2019).

38. Christensen, P. R., Scheuermann, A. M., Loeffler, K. E. & Helms, B. A. Closed-loop recycling of plastics enabled by dynamic covalent diketoenamine bonds. *Nat. Chem.* **11**, 442–448 (2019).

39. Song, Y. et al. Advancing the development of highly-functionalizable glucose-based polycarbonates by tuning of the glass transition temperature. *J. Am. Chem. Soc.* **140**, 16053–16057 (2018).

40. Sangroniz, A. et al. Packaging materials with desired mechanical and barrier properties and full chemical recyclability. *Nat. Commun.* **10**, 3559–3565 (2019).

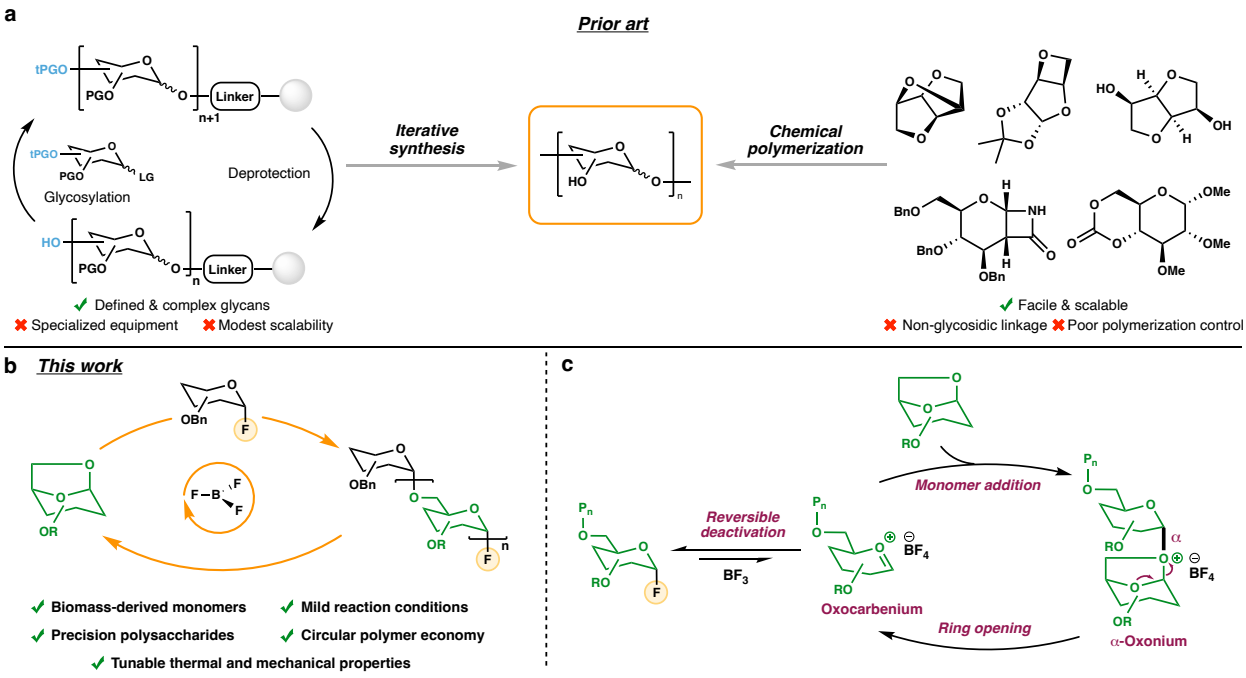

Fig. 1 | Living cationic ring-opening polymerization of 1,6-anhydrosugars. a, Established pathways to polysaccharides. **b**, Representative reaction scheme of living cationic ring-opening polymerization of 1,6-anhydrosugars in this work. **c**, Proposed mechanism. LG, leaving group; PG, protecting group; tPG, temporary protecting group; Bn, benzyl; Me, methyl; R, alkyl/allyl group.

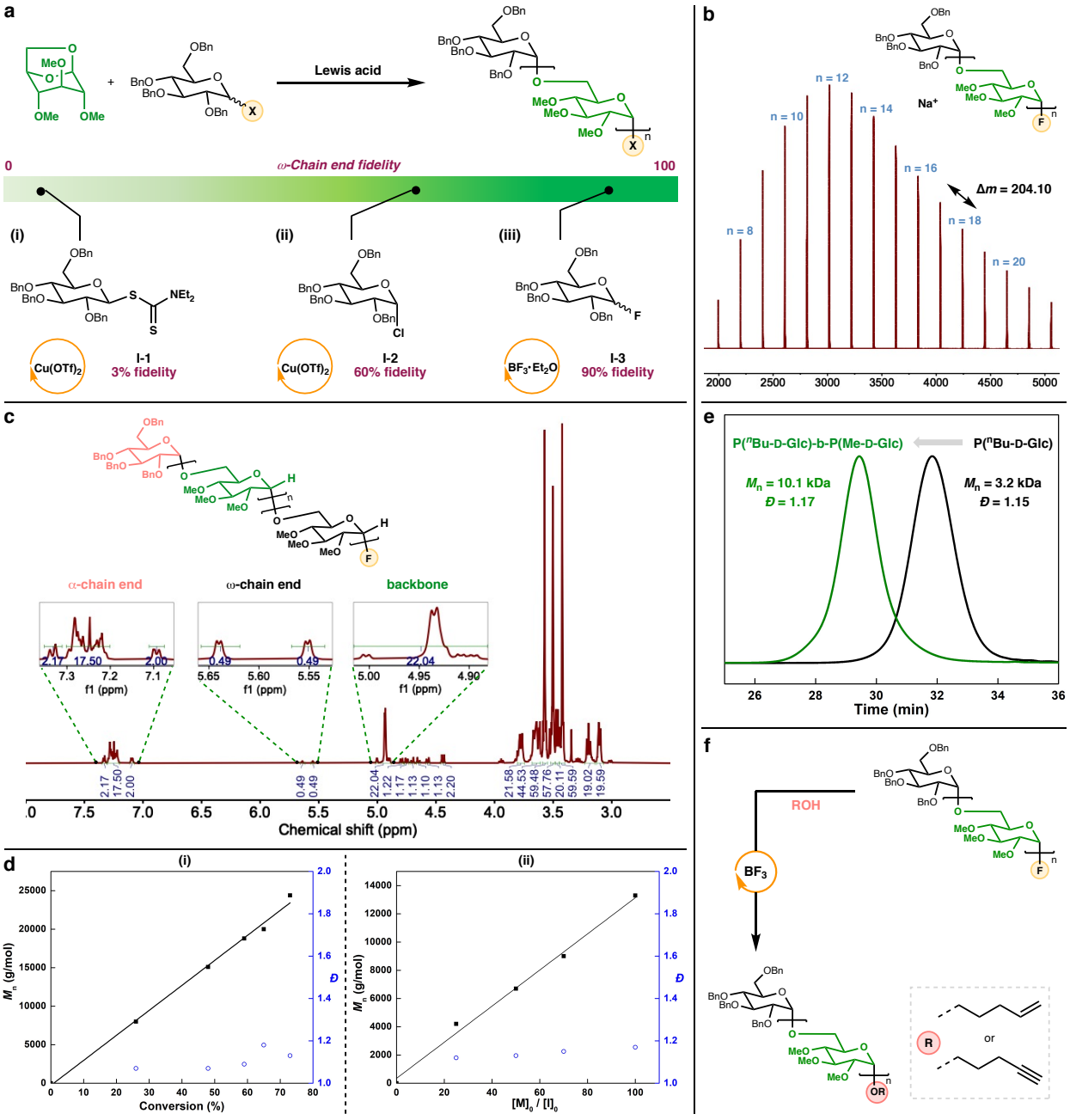

Fig. 2 | Preparation and characterization of precision polysaccharides. a, Development of living CROP of 1,6-anhydrosugars. **b**, MALDI-TOF MS spectrum of **P(Me-D-Glc)**. **c**, ^{1}H NMR spectra of **P(Me-D-Glc)**. **d**, (i) Plots of M_n and $Đ$ as a function of monomer conversion and (ii) Plots of M_n and $Đ$ as a function of the $[M]_0/[I]_0$ ratio. **e**, Synthesis of block copolysaccharide **P(*n*Bu-D-Glc)-*b*-P(Me-D-Glc)**. **f**, Chain end modification of **P(Me-D-Glc)**. Et, ethyl; *n*Bu, *n*-butyl; Glc, glucose; OTf, trifluoromethanesulfonate.

a

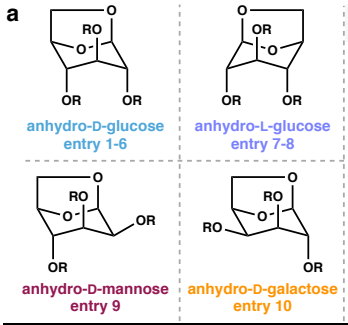

Entry	R	$[M]_0:[I]_0$	Conversion	$M_{n,Theo}$ (kDa)	$M_{n,NMR}$ (kDa)	$M_{n,GPC}$ (kDa)	$Đ$
1	Me	50	80%	8.7	9.5	5.8	1.23
2	Et	400	57%	56.6	46.0	32.2	1.34
3	^{n}Pr	100	75%	22.1	22.1	16.7	1.38
4	^{n}Bu	100	81%	27.3	24.0	18.1	1.13
5	^{n}Pen	100	76%	28.8	25.1	18.6	1.16
6	All	10	73%	2.6	2.5	2.6	1.18
7	^{n}Bu	100	80%	27.0	25.6	18.5	1.21
8	All	10	74%	2.6	2.5	2.6	1.17
9	All	15	80%	3.9	3.9	3.3	1.24
10	Et	50	70%	9.1	8.4	6.4	1.14

b

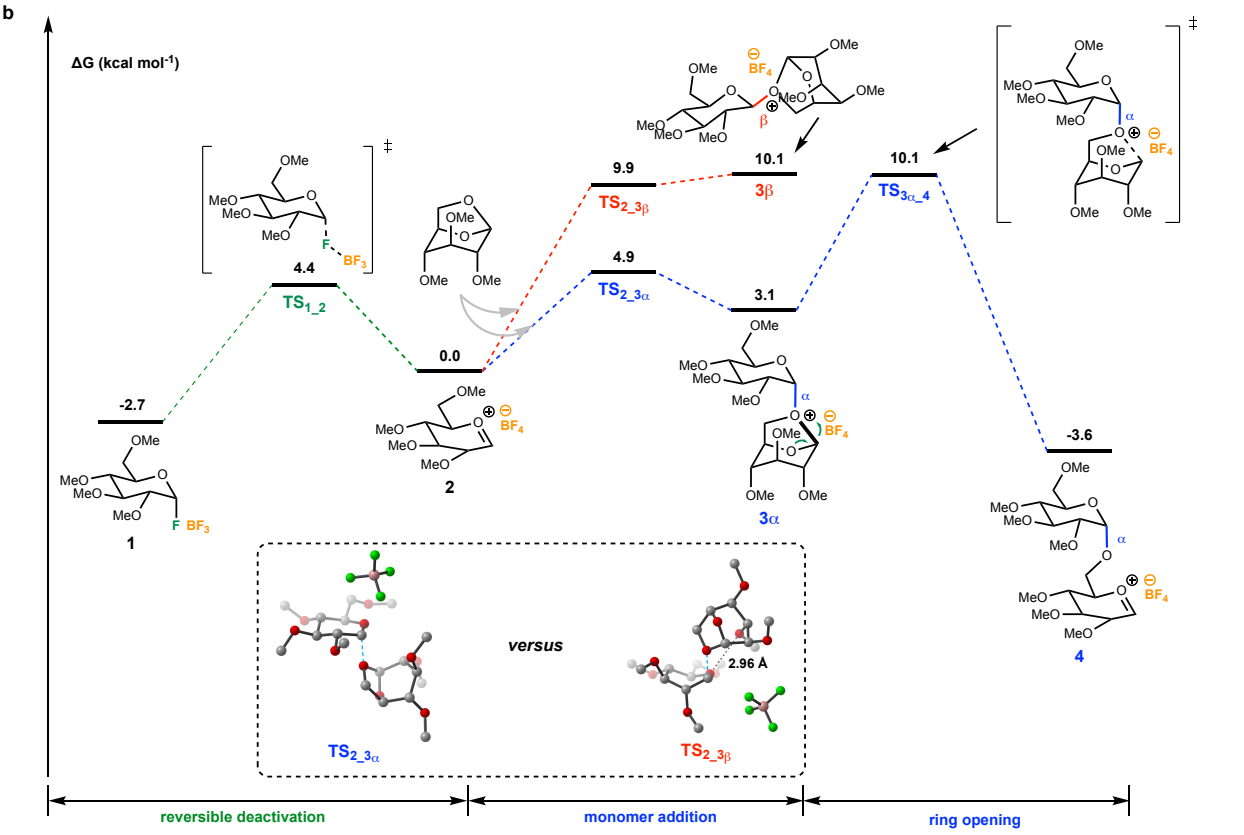

Fig. 3 | Monomer scope and computational studies. a, Monomer scope: polymerization reactions were performed at 25 ºC in dichloromethane for six hours; more experimental details are provided in Supplementary Information. **b**, Energy profile of reversible deactivation and propagation process. Free energies (kcal mol^{-1}) are obtained at the level of ωB97X-2-D3(BJ)/ma-def2-TZVPP-def2-TZVPP/SMD(DCM)//B3LYP-D3(BJ)/ma-def2-SVP-def2-SVP/PCM(DCM). The DFT calculations were performed starting from a methyl-protected glucosyl fluoride **1** to mimic the dormant species during living CROP and simplify the calculations. ^{n}Pr, *n*-propyl; ^{n}Pen, *n*-pentyl; All, allyl.

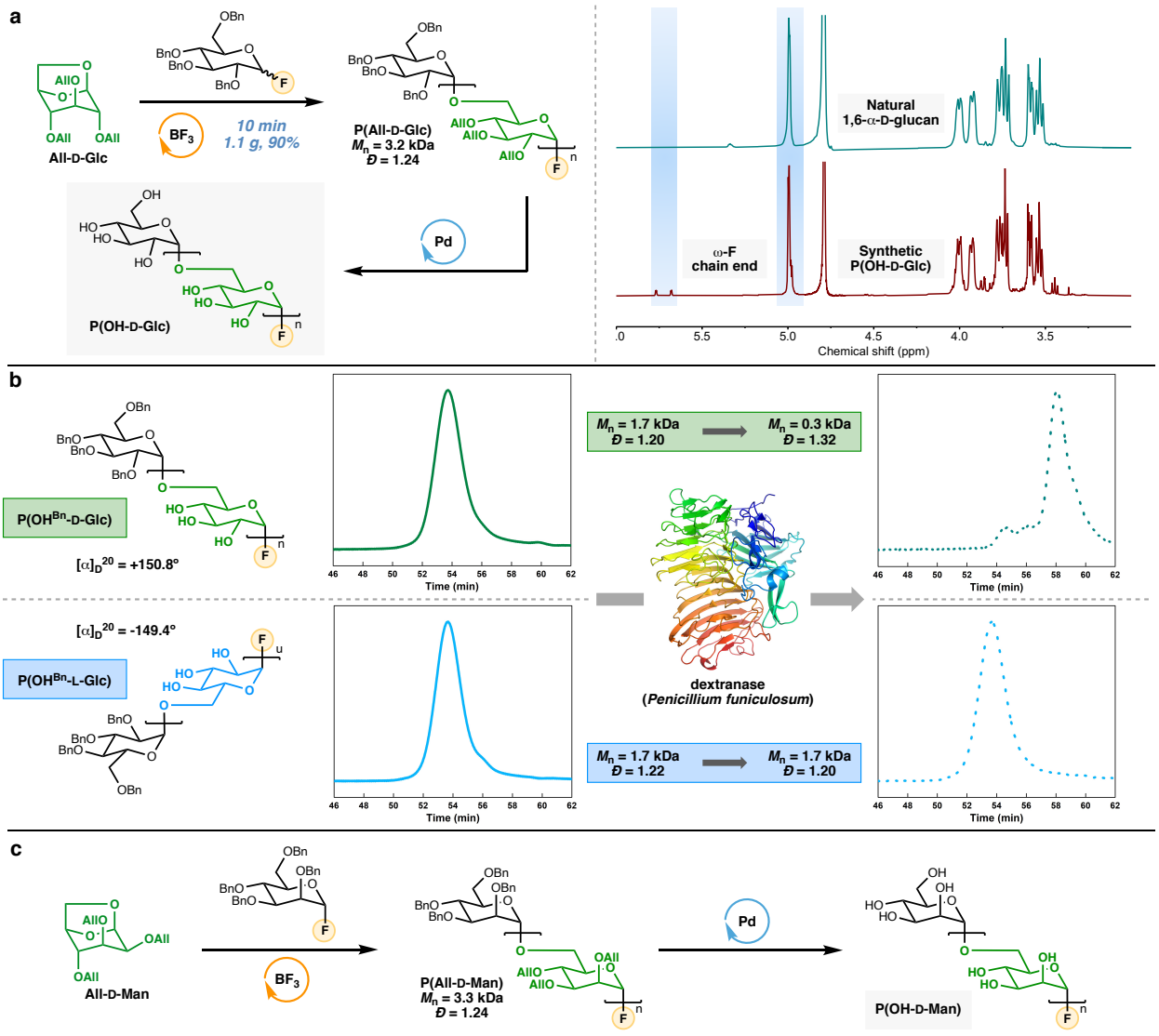

Fig. 4 | Synthesis of biologically relevant precision polysaccharides. a, Synthesis of α-1,6-D-glucan **P(OH-D-Glc)** and comparison to natural α-1,6-D-glucan. **b**, Enzymatic degradation studies of **P(OH^{Bn}-D-Glc)** and **P(OH^{Bn}-L-Glc)**. **c**, Synthesis of α-1,6-D-mannan **P(OH-D-Man)**. Pd, $Pd(PPh_3)_4$ and $Pd(OH)_2$; Man, mannose.

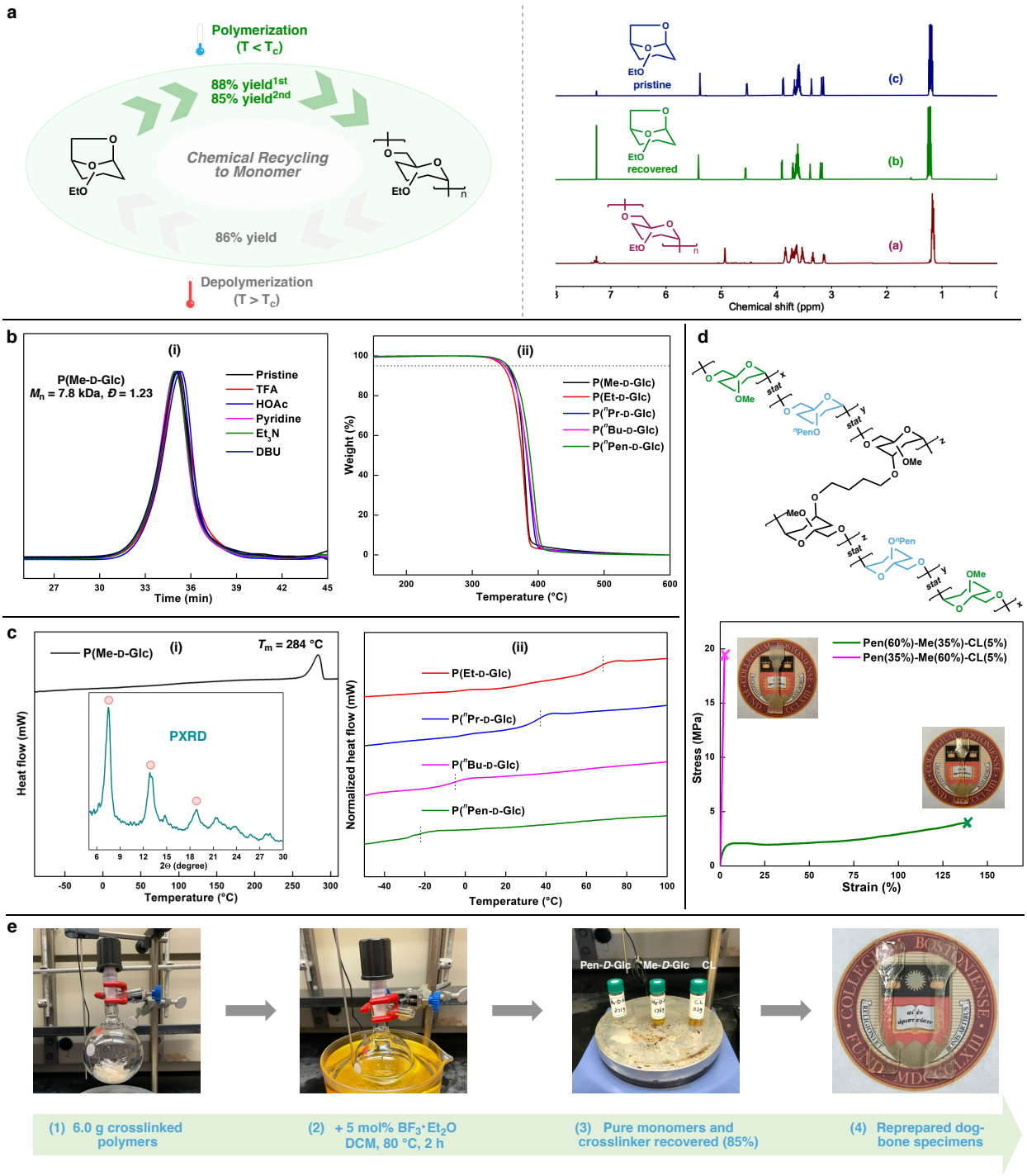

Fig. 5 | Chemical recycling and material properties of precision polysaccharides. a, Polymerization-depolymerization cycles. **b**, (i) SEC trace overlays of **P(Me-D-Glc)** treated by various additives and (ii) TGA curves of **P(R-D-Glc)** (**R** = **Me**, **Et**, **nPr**, **nBu**, **nPen**). **c**, (i) DSC curve and powder XRD profile (inset) of **P(Me-D-Glc)** and (ii) overlays of DSC curves of **P(R-D-Glc)** (**R** = **Et**, **nPr**, **nBu**, **nPen**). **d**, Stress-strain curves of **PN1** (green) and **PN2** (magenta). **e**, Depolymerization of materials and reprepared materials **PN1'** and **PN2'** from recovered monomers.

Methods

In a glovebox under a nitrogen atmosphere, an oven-dried vial was charged with [M], [I] and DCM (or $CDCl_3$), BF_3•Et_2O was added. After 6 hrs, the reaction vial was removed from the glovebox and quenched with two drops of methanol. The polymer solution was precipitated into cold hexane or MeOH/H_2O (v/v, 1/1), centrifuged, discarded the solvent, and redissolve in $CHCl_3$. This procedure was repeated three times to ensure any catalyst residue or unreacted monomer was removed. The polymer was dried under high vacuum overnight to a constant weight.

Data availability

All data supporting the findings of this study are available within the article and its Supplementary Information.

Acknowledgements

This work was supported by the Arnold and Mabel Beckman Foundation through a Beckman Young Investigator Award to J.N. and the National Science Foundation Major Research Instrumentation (NSF-MRI) Program, under the award number CHE-2117246. We thank J. B. Matson, S. Blosch, M. J. Zhong, M. X. Cao, C. F. Ke, Q. M. Lin, T. S. Emerick, T. Goodwin, M. W. Grinstaff, S. EI-Arid, M. Zhou, C. J. Yang, C. Liu, T. Jayasundera, M. Domin, S.-Y. Liu, J. A. Byers, and J. Morken for characterization assistance and helpful discussions.

Author contributions

L.W. and J.N. conceived and designed the project. J.N. oversaw the project. L.W., S.R., and Z.Zhao performed the experiments. Z.Zhou performed the computational studies. D.S., J.Z. and J.W. performed tensile testing. All authors discussed the results and commented on the manuscript.

Competing interests

A provisional patent based on this work has been filed by Boston College.